Optical characteristic of sol-gel synthesized lead lanthanum titanate-cobalt iron oxide multiferroic composite thin film

Subhasis Roy and S. B. Majumder

Citation: Journal of Applied Physics **112**, 043520 (2012); doi: 10.1063/1.4747918
View online: http://dx.doi.org/10.1063/1.4747918
View Table of Contents: http://scitation.aip.org/content/aip/journal/jap/112/4?ver=pdfcov
Published by the AIP Publishing

Optical characteristic of sol-gel synthesized lead lanthanum titanate-cobalt iron oxide multiferroic composite thin film

Subhasis Roy and S. B. Majumder[a)]
Materials Science Centre, Indian Institute of Technology, Kharagpur—721302, India

(Received 21 March 2012; accepted 20 July 2012; published online 31 August 2012)

In the present work, we have investigated the optical characteristics of $(1-x)$ $Pb_{0.85}La_{0.15}TiO_3$ (PLT15)-x $CoFe_2O_4$ (CFO) (x, volume fraction of CFO $0.0 \leq x \leq 0.12$) composite multiferroic thin films. It has been demonstrated that the analysis of wavelength dispersion of refractive indices is an effective tool to comment on the magnetostrictive (CFO) phase distribution in perovskite (PLT15) matrix. Thus, in case of 0-3 type $(1-x)$ PLT15-x CFO composite films, it has been demonstrated that as long as CFO phase is distributed homogeneously in PLT15 matrix, the measured refractive indices follow Sellmeir dispersion formalism. Interestingly, for percolative magnetostrictive phase (CFO) distribution, the refractive index variation of the composite films deviates from the Sellmeir type dispersion. Absorption coefficient and the band gap energy are estimated for PLT15 and $(1-x)$ PLT15-x CFO composite films with varying CFO volume contents. Both refractive indices and packing fraction of $(1-x)$ PLT15-x CFO composite films are found to be marginally reduced with the increase in CFO volume contents. The band gap of these films is found to be systematically reduced with the increase in CFO volume contents. The change in band gap is argued to be due to cation/(s) diffusion across PLT15 and CFO interface. © *2012 American Institute of Physics*. [http://dx.doi.org/10.1063/1.4747918]

I. INTRODUCTION

Multi-ferroic composite thin films are now-a-days being studied with renewed interest for their possible use in various microelectronic and integrated optic devices. The family of optically transparent lanthanum doped lead titanate (viz. $Pb_{0.68}La_{0.32}TiO_3$) and lead zirconate titanate (viz. $Pb_{0.68}La_{0.32}Zr_{0.65}Ti_{0.35}O_3$) materials have found applications in optical devices for optical storage, protective limiters, and spatial light modulators.[1] The studies of optical properties of thin films are important both as diagnostic tools of thin film quality and for possible device applications. The evaluation of optical dispersions and other relevant optical constants of magneto-electric composites thin films are of considerable importance for applications in integrated optics. The refractive index and the extinction coefficients of the electroptic films are considered to be the key parameter for device design.[2,3] Optical characterizations have also found to be useful in determining the band gap of transparent electro-ceramic thin films.

As compared to transparent ferroelectric thin films, very few reports are available on the optical properties of (single phase) multiferroic thin films.[4–6] As for example, Shima *et al*. recently reported the optical constants and band gap of sol-gel derived $BiFeO_3$ and pulsed laser deposited (PLD) $(Bi,Nd)(Fe,Mn)O_3$ (BNFM) films.[7,8] Choi *et al*. reported the photovoltaic effect of $BiFeO_3$.[8,9] To the best of our knowledge, so far the detailed optical characteristics of 0–3 type multiferroic composite films have not been reported in open literature.

High optical transparency ($\geq$70%) in the visible wavelength region, high refractive index (n), and low extinction coefficient (k) are desirable for thin films for their use in optical devices. Hence, the measurement of these parameters is helpful in determining their relevance to possible device applications. Moreover, characterization of films in terms of optical parameters may also be useful as a diagnostic tool to evaluate phase content and structural parameters such as film thickness, thickness uniformity, packing fraction, and surface roughness of the multiferroic composite thin films.

In our earlier papers, we have discussed the optimization of the processing parameters to obtain excellent quality PLT15 and $(1-x)$ PLT15-x CFO composite thin films. The phase formation behavior, microstructural evaluation, electrical, magnetic, and magneto-electric characteristics of these films have also been reported.[10,11] In this paper, we have studied the optical properties of PLT15 and $(1-x)$ PLT15-x CFO composite films. The variation of optical constants has been correlated with the CFO volume contents in these films. We have also demonstrated that the optical characterization could be an effective diagnostic tool to determine the thickness, surface roughness, and density of these films.

To determine optical constants of PLT15 and $(1-x)$ PLT15-x CFO composite thin films, we have used the "envelope method" originally developed by Manifacier *et al*.[12] The details of this have been provided as supplemental information.[19] The brief outline of this method is described as follows. The "envelop method" has been used by several researchers to determine optical constants of various insulating and semi-insulating thin films.[12–14] It is only applicable in the wavelength region where the optical transmittance is more than 40%. Using this method, the refractive index (n), extinction coefficient (k), and film thickness (d) of

[a)]Author to whom correspondence should be addressed. Electronic mail: subhasish@matsc.iitkgp.ernet.in. Tel.: +91-3222-283986 (O) +91 9433611775.

the films are calculated from the transmission spectra. The packing density of each film is derived from its refractive index. The surface roughness of each film is qualitatively estimated from the extinction coefficient. In the strong absorption region, the optical constants are estimated from the reflectance data. Using transmittance and reflectance data in strong absorption region, the absorption coefficient (α) has been calculated from the estimated extinction coefficient (k). Finally, the band gap energy (E_g) has been calculated from the absorption coefficient (α).

II. EXPERIMENTAL

We have synthesized $(1-x)$ $Pb_{0.85}La_{0.15}TiO_3$—x $CoFe_2O_4$ ($(1-x)$ PLT15-x CFO) ($0.0 \leq x \leq 0.12$) composite thin films on single crystalline (0001) sapphire substrates using a sol-gel route. To prepare PLT15 precursor sol, lead acetate tri-hydrate ($Pb(CH_3COO)_2$ $3H_2O$), lanthanum nitrate hexahydrate ($La(NO_3)_3$ $6H_2O$), and titanium butoxide [$Ti(OC_4H_9)_4$] are used as precursor materials. Lead acetate tri-hydrate and lanthanum nitrate co-dissolved in warm acetic acid through continuous stirring. In a separate three-neck flask, stoichiometric titanium butoxide was dissolved in glacial acetic acid (in 1:2 molar ratio) to reduce the moisture sensitivity of the alkoxide precursor. The chelated sol thus prepared was added drop by drop to the mixed solution of lead acetate tri-hydrate and lanthanum nitrate (through continuous stirring for 15–20 min) to prepare PLT15 precursor sol. Cobalt(II) nitrate hexahydrate ($Co(NO_3)_2.6H_2O$) and iron (III) nitrate nonahydrate ($Fe(NO_3)_3$ $9H_2O$) were used to prepared 0.25 M $CoFe_2O_4$ precursor sol. These two salts were dissolved into acetic acid and mixed together in 1:2 molar ratios. To prepare $(1-x)$ PLT15-x CFO composite precursor sol, 0.25 M PLT15 and 0.25 M CFO precursor sol were mixed in 100:0, 99:1, 97:3, 95:5, 92:8, and 90:10 volume ratio, respectively, through continuous stirring for 30 min at room temperature. The respective nominal volume fraction of crystalline CFO in the composite films is calculated to be 0.0, 0.018, 0.036, 0.059, 0.082, and 0.117, respectively.

Sapphire single crystals (0001) were cleaned ultrasonically, first in a series of organic solvents and finally with absolute alcohol. The cleaned substrates were dried in nitrogen flow. The precursor sol was spun coated on cleaned sapphire substrates at 3000 rpm for 10 s. Just after deposition, the films were directly inserted in a preheated furnace at 400 °C and heated for 5 min in air for the removal of organics followed by quenching in ambient air. The coating and firing steps were repeated for 10 times to increase the film thickness. After the firing of the final coating, the furnace temperature was increased (at the rate of ~10 °C/min) to 700 °C and the films were annealed for 1 h followed by cooling them down to room temperature using normal furnace cooling.

The annealed films were characterized in terms of their phase formation behavior and microstructure evaluation using an x-ray diffractometer and field emission scanning electron microscope, respectively. The transmission and reflection spectra are recorded using an UV-VIS scanning spectrophotometer. The transmission spectra of PLT15 and $(1-x)$ PLT15-x CFO composite thin films are measured using air as reference. The reflectances of these thin films were measured with respect to a standard sample having 100% reflectance. During the measurements, the range of wavelength scanned was 200–900 nm at a scanning rate of 200 nm/min and sampling interval of 5 nm.

III. RESULTS AND DISCUSSION

A. Phase formation behavior and microstructure characteristics

The phase formation behavior of PLT15 and $(1-x)$ PLT15-x CFO composite films on sapphire substrates are found to be similar to that reported for these films on platinized silicon substrates.[10,11] Thus, Fig. 1(a) shows the XRD patterns of PLT15 and $(1-x)$ PLT15-x CFO composite films on sapphire substrate. The XRD peaks corresponding to the perovskite (PLT15) phases are readily identified, however peaks corresponding to the CFO phase is hard to find. This could be due to the nano-scale distribution of CFO phase in PLT15 matrix. The constituent cation/(s) from CFO

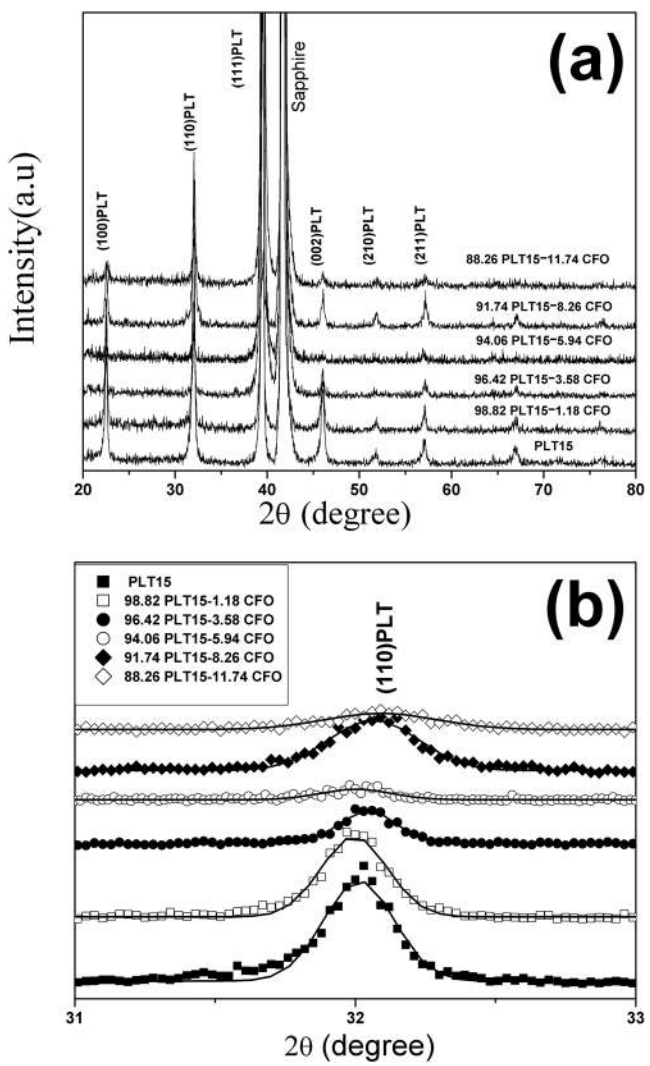

FIG. 1. (a) XRD patterns of PLT15 and $(1-x)$ PLT15-x CFO composite films on sapphire substrate. (b) Slow scanned (110) x-ray diffraction peaks.

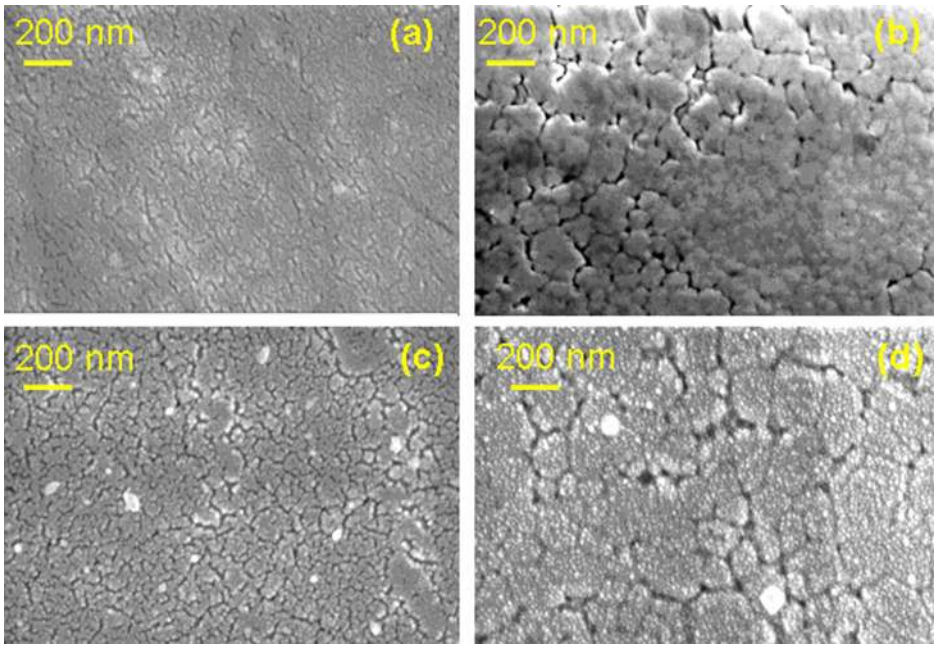

FIG. 2. Surface morphologies of (a) PLT15, (b) 96.4 PLT15-3.6 CFO, (c) 94.06 PLT15 – 5.94 CFO, and (d) 88.26 PLT15 – 11.74CFO composite thin films on transparent sapphire (0001) substrates.

phase probably diffuse to PLT15 lattice resulting the shift of its diffraction peaks. Thus, as shown in Fig. 1(b), a systematic shift is apparent in the most intense (110) diffraction peak of the perovskite phase with the increase in CFO volume content. Similar observation is also reported for $(1-x)$ PLT15-x CFO composite films deposited on platinized silicon substrates.

Figure 2 compares the surface morphologies of (a) PLT15 (b) 96.4 PLT15-3.6 CFO, (c) 94.06 PLT15 – 5.94 CFO, and (d) 88.26 PLT15 – 11.74CFO composite thin films on transparent sapphire (0001) substrates. PLT15 film exhibits uniform nano-size grain. At lower magnification, all the films checked to be crack-free. The rosette types of grains are apparent in Figs. 2(b) and 2(d). For Figs. 2(a) and 2(c), sinuous and continuous channels are observed throughout the surface of the films. Energy dispersive spectroscopy (EDS) analyses on the composite films confirm the presence of all the constituent cations including Pb, La, Ti, Co, and Fe; however from the surface morphology, we could not identify individual grains of PLT15 or CFO unequivocally.

B. Optical characteristics of (1 – X) PLT15 – XCFO composite films

In our earlier publications, it was reported that for $(1-x)$ PLT15-x CFO composite films (deposited on platinized silicon substrates), the measured dielectric constant and loss tangent initially increase and maximize at certain specific CFO volume contents and then both these parameters are decreased steadily.[10,11] We have demonstrated that the increase of dielectric constant and loss tangent fits well to general empirical equations (of the respective parameters), developed originally for percolative ceramic: metal composites. At the percolation threshold (~8.6 vol. % of CFO contents, derived from non-linear curve fitting of those empirical equations), both the dielectric constant and loss tangent of $(1-x)$ PLT15-x CFO composite film is found to be increased significantly as compared to pure PLT15 thin film. Beyond the percolation threshold, the sharp drop in dielectric constant with the increase in CFO volume contents is thought to be related to the sudden drop in the resistivity of the composite films.

In the present paper, these composite films deposited on single crystalline sapphire substrates are characterized in terms of their optical properties. Figure 3 shows the typical transmittance and reflectance spectra of the synthesized films. The transmission spectrum can be subdivided into three distinct regions namely weak ($T \geq 0.6$), medium ($0.6 \geq T \geq 0.4$), and strong absorption region ($T \leq 0.4$). To estimate the optical constants, the envelop method is applied only in weak and medium absorption regions. The refractive index (n) of the deposited film as a function of the incident photon wavelength (λ) is calculated using the following relation:

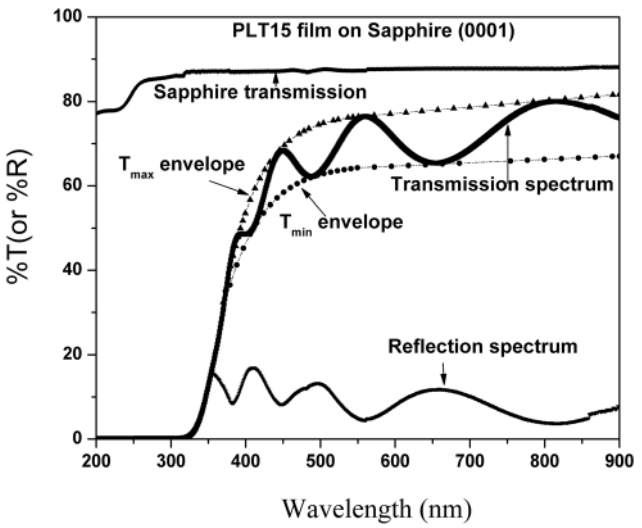

FIG. 3. Transmittance and reflectance spectra and the T_{max} and T_{min} envelopes for undoped PLT film on a completely transparent sapphire (0001) substrate.

$$n=[N'+(N'^2-n_s)^{0.5}]^{0.5}, \quad (1)$$

where

$$N'=0.5(1+n_s^2)+[2n_s[(T_{max}-T_{min})/T_{max}T_{min}]].$$

The refractive index (n_s) of sapphire substrate as a function of photon wavelength (λ) can be calculated using the following empirical dispersion relation:

$$n_s^2=1+[A\lambda^2/(\lambda^2-\lambda_1^2)]+[B\lambda^2/(\lambda^2-\lambda_2^2)]+[C\lambda^2/(\lambda^2-\lambda_3^2)], \quad (2)$$

where $A=1.023798$, $B=1.058264$, $C=5.280792$, $\lambda_1=0.00377588$, $\lambda_2=0.0122544$, $\lambda_3=321.3616$, and λ is in μm.

Hence using values of maxima and minima in the transmittance spectrum, one can obtain the refractive index (n) of the film as a function of λ.

Figure 4(a) shows the plot of refractive index (n) as a function of photon wavelength (λ) for PLT15 and $(1-x)$ PLT15-x CFO composite thin films with various CFO volume contents. At He-Ne laser wavelength of $\lambda=632.8$ nm (denoted by vertical dotted line), it is seen that the refractive index value of PLT15 thin film (~ 2.32) is very close to that reported in literature.[15] With the increase in CFO volume contents, the refractive indices of the composite films are found to be decreased systematically. Table I summarizes the value of the optical constants obtained in the present study. The decrease in the refractive indices may be due to the nano-scale distribution of CFO phase in PLT15 matrices. The data of the refractive $n(\lambda)$ as a function of wavelength (λ) can be fitted to a Sellmeier type dispersion equation, assuming that the material is composed of individual dipole oscillators, which are set to force vibrations by incident light. Domenico and Wemple[16] proposed that for semiconducting and insulting materials, the lowest energy oscillator as the largest contributor to *"n"* and a single term Sellmeier relation could adequately describe the wavelength dispersion of refractive index. The relevant dispersion relation can be written as

$$n^2(\lambda)-1=\frac{S_0\lambda_0^2}{[1-(\lambda_0/\lambda)^2]}, \quad (3)$$

where S_0 is an average oscillator strength and λ_0 is an average oscillator wavelength. A plot of $(n^2-1)^{-1}$ versus $(1/\lambda)^2$ yields a straight line and the parameters *So* and λo can be obtained from the slope $(1/S_o)$ and intercept $(1/S_o\lambda_o^2)$ of the line. Knowing the values of *So* and λ_o, the energy of the oscillator $Eo=hc/\lambda_o$ (where $h=$ Planck's constant and c is the velocity of light) and the refractive index dispersion parameter (E_o/S_o) are determined.

In accordance to the single term Sellmeir dispersion formula for one dominant electronic oscillator, the function $(n^2-1)^{-1}$ is plotted vs. λ^{-2}. Figure 4(b) shows such plots (symbols) and linear fit (solid lines following Eq. (3)) for PLT15 and all $(1-x)$ PLT15-x CFO composite films. As shown in Fig. 4(b) for PLT15 as well as $(1-x)$ PLT15-x CFO composite films with dilute CFO volume contents, the data fit well according to Eq. (3). For films with CFO volume contents in the vicinity or higher than the CFO percolation threshold (~8.6 vol. %), either the quality of linear fit deteriorates or does not fit at all. These optical data suggest that analysis of multiferroic composite films in terms of its dispersion of refractive indices could be an effective tool to comment on the magnetostrictive phase distribution in perovskite matrix. Thus in case of 0–3 type $(1-x)$ PLT15-x CFO composite films, we have demonstrated that as long as CFO phase is distributed homogeneously in PLT15 matrix, the measured refractive indices follow Sellmeir dispersion formalism. Interestingly, when the percolation of the magnetostrictive phase (CFO) initiates, then the variation of refractive indices deviates from the Sellmeir type dispersion (for one dominant electronic oscillator).

For PLT15, the typical values of S_o, λ_o, energy of the oscillator $E_o=hc/\lambda_o$ (where $h=$ Planck's constant and c is the velocity of light) and the refractive index dispersion parameter (E_o/S_o) are estimated to be $1.47832\times10^{14}/m^2$, 0.166376 μm, 7.45598 eV, and 5.04355×10^{-14} eV/m^2, respectively. The

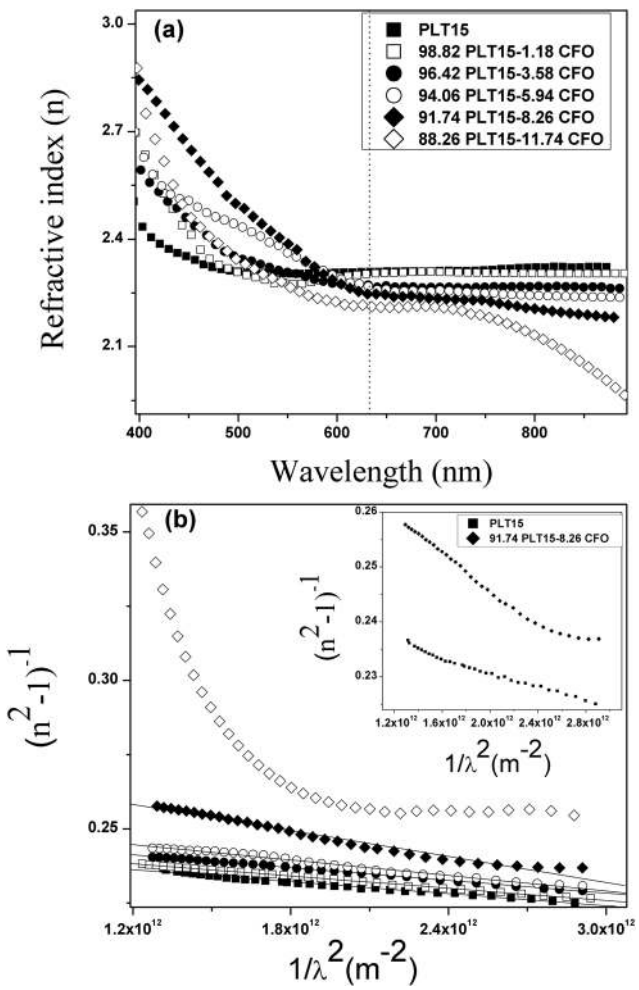

FIG. 4. (a) Plot of refractive index (n) as a function of photon wavelength (λ) for PLT15 and $(1-x)$ PLT15-x CFO composite thin films with various CFO volume contents. (b) plots (symbols) and linear fit (solid lines following Eq. (3)) for PLT15 and all $(1-x)$ PLT15-x CFO composite films. The variation of $(n^2-1)^{-1}$ vs $1/\lambda^2$ for PLT15 and 91.74PLT15 − 8.26 CFO thin films are shown separately in the inset.

TABLE I. Summary of the optical result of (1 − x) PLT15-x CFO composites thin films.

Composition	Thickness (d_{fav}) (nm)	n (at 632.8 nm)	k (at 632.8 nm)	f %	E_g (eV)
PLT15	421.5	2.31	0.01779	78.79	3.62
98.82 PLT15-1.18 CFO	258.57	2.3	0.02505	78.41	3.59
96.42 PLT15-3.58 CFO	236.41	2.27	0.03632	78.4	3.55
94.06 PLT15-5.94 CFO	198.07	2.25	0.0352	78.41	3.52
91.74 PLT15-8.26 CFO	190.47	2.24	0.03673	78.41	3.48
88.26 PLT15-11.74 CFO	174.16	2.21	0.07906	74.38	3.43

refractive index dispersion parameter compares well with that of the model of Domenico and Wemple,[16] which states that its value should be smaller than $(6 \pm 0.6) \times 10^{-14}$ eV/m^2 owing to the contribution of Pb^{2+} in lead based solid solutions (viz. PZT). The validity of a single oscillator model for such multiferroic composite film is not beyond doubt. Hence, parameters values S_o and λ_o need only be considered as approximate guide and their use for comparing the thin films characteristics should be done judiciously. Irrespective of this fact, we have observed interesting variation of these parameters in (1 − x) PLT15-x CFO composite films as tabulated in Table II. We are making and attempt to explain the salient features of this variation. The PLT15 as well as (1 − x) PLT15-x CFO composite films have been considered to be composed of individual dipole oscillators, which are set to force vibrations by incident light. Among these oscillators, the lowest energy one is assumed to be the largest contributor to the refractive indices (n). As shown in Table II, the average oscillator strength (S_o) is reduced, whereas the average oscillator wavelength is systematically increased with the increase of CFO volume contents in (1 − x) PLT15-x CFO composite films. As mentioned earlier, the $(n^2-1)^{-1}$ vs λ^{-2} variation could not be fitted according to Sellmeir dispersion for (1 − x) PLT15-x CFO (11.74 vol. %) composite film. It is plausible that the average oscillator strength (of perovskite dipolar phase) is reduced due to the nano-scale distribution of magnetostrictive (CFO) phase; and as the CFO volume contents increase, the strength of the oscillation is reduced. Interestingly, the value of S_o is lowest in the vicinity of the percolation threshold of the CFO phase and the $(n^2-1)^{-1}$ vs λ^{-2} variation start to deviate from the linearity. When the CFO volume contents are beyond the percolation threshold, then the linear relation is not followed at all (see Fig. 4(b)). The distribution of CFO phase is also reflected in the increase of the average oscillator wavelength (λ_o) with the increase in CFO volume contents. Since λ_o is progressively increased, as expected, the energy of the oscillator ($E_o = hc/\lambda_o$) is decreased. As mentioned earlier, the refractive index dispersion parameter is the ratio of E_o/S_o. As plotted in the inset of Fig. 4(b), it is interesting to note that the variation of the parameter $(n^2-1)^{-1}$ is increased appreciably with the increase in CFO volume contents. The wavelength dispersion of the estimated refractive indices with the increase of CFO volume contents (especially, beyond the percolation threshold) is more distinctly observed in Fig. 4(a). The analyses presented above clearly demonstrate that the study of the wavelength dispersion of the refractive indices could be an effective diagnostic tool to investigate the nature of magnetostrictive phase distribution in perovskite matrices for such 0–3 type composite films with dilute magnetostrictive phase contents.

The very occurrence of interference fringes points to the homogeneity of thickness in the films. The thickness can be calculated with precision as described earlier if the refractive index corresponding to adjacent maxima or minima is known. Table III shows the calculations for PLT15 and (1 − x) PLT15-x CFO composite films. The accuracy in thickness values is significantly increased by this method. As shown in Table III, the thickness obtained from our optical measurements match reasonably well with the thickness values obtained by other commercial thickness measuring equipment. Although the films are prepared using identical number of coating cycles, the range of thickness of final annealed films varies from 174 to 421 nm. This could be due to the difference in precursor chemistries in PLT15 and CFO precursor sols used for deposition.

The thickness values are used to calculate the extinction coefficient (k) as a function of λ for all the films. Figure 5 shows the plot of (k) as a function of (λ) for PLT15, and (1 − x) PLT15-x CFO composite thin films. The extinction coefficient of PLT15 thin film (at 632.8 nm) is in the order of 10^{-2} and it increases with the increase of CFO volume contents in (1 − x) PLT15-x CFO composite films. The order of extinction coefficient larger than that reported for metalorganic chemical vapor deposition (MOCVD) grown film. Recall, we

TABLE II. The estimated dispersion parameters (So, λo, Eo, and Eo/So) for all thin film compositions.

Composition	S_0 (10^{14} m^{-2})	λ_0 (μm)	Eo (eV)	E_0/S_0 (10^{-14} eV m^2)
PLT15	1.47832E14	0.166376	7.45598	5.04355
98.82 PLT15-1.18 CFO	1.45024E14	0.167248	7.41711	5.11439
96.42 PLT15-3.58 CFO	1.39277E14	0.169517	7.31787	5.25419
94.06 PLT15-5.94 CFO	1.15043E14	0.184578E	6.72073	5.84192
91.74 PLT15-8.26 CFO	6.84051E13	0.2.30237	5.38793	7.87651
88.26 PLT15-11.7 CFO	Not fitted	Not fitted	Not fitted	Not fitted

TABLE III. Computation of the thickness of (1 − x) PLT15-x CFO composites thin films (p-peak position and v-valley position).

Composition	Wave length (nm)	n	d′(nm)	d'_{av} (nm)	m′	m	d_f (nm)	$d_{f\ av}$ (nm)	$d_{filmetrics}$ (nm)
PLT15	391(P)	2.49	436.37	425.08	5.41	5	392.57	421.5	460.65
	450(P)	2.35	484.12		4.43	4	382.97		
	549(P)	2.30	380.83		3.56	4	477.39		
	810(P)	2.33			2.44	2	347.63		
	406(V)	2.42	401.18		5.06	4.5	377.47		
	490(V)	2.31	422.94		4.01	4.5	477.27		
	654(V)	2.31			3.01	3.5	495.45		
98.82 PLT15-1.18 CFO	374(P)	2.86	235.5	270.53	4.13	4	261.5	258.5	297.72
	440(P)	2.43	311.48		2.98	3	271.6		
	582(P)	2.28			2.11	2	255.26		
	397(V)	2.73	232.14		3.72	3.5	254.48		
	487(V)	2.30	303.01		2.55	2.5	264.67		
	748(V)	2.30			1.66	1.5	243.91		
96.42 PLT15-3.58 CFO	377(P)	2.8	246.61	233.44	3.46	3	201.96	236.4	275.56
	463(P)	2.5	218.46		2.52	3	277.8		
	780(P)	2.43			1.45	1	160.49		
	396(V)	2.62	235.26		3.08	3.5	263.49		
	550(V)	2.47			2.09	2.5	278.34		
94.06 PLT15-5.94 CFO	368(P)	3.1	155.7	208.02	3.51	4	237.41	198.0	237.22
	470(P)	2.45	206.93		2.13	2	191.83		
	801(P)	2.24			1.14	1	178.79		
	410(V)	2.51	261.45		2.5	2.5	204.18		
	563(V	2.37			1.72	1.5	178.16		
91.74 PLT15-8.26 CFO	380(P)	2.88	188.04	206.11	3.12	3	197.91	190.4	229.62
	500(P)	2.46	222.29		2.02	2	203.25		
	820(P)	2.19			1.1	1	187.21		
	413(V)	2.75	208.01		2.74	2.5	187.72		
	557(V)	2.37			1.75	1.5	176.26		
88.26 PLT15-11.74 CFO	433(P)	2.85	177.6	187.09	2.46	2	151.92	174.1	213.31
	592(P)	2.23			1.4	1	132.73		
	480(V)	2.55	196.59		1.98	1.5	141.17		
	780(V)	2.16			1.03	1.5	270.83		

have synthesized PLT15 as well as (1 − x) PLT15-x CFO composite films using a hybrid sol-gel technique using alkoxide precursor only for titanium. For other constituent elements (such as lead, lanthanum, cobalt, and iron), respective salts are used as precursor materials. This could be one of the reasons to yield relatively rougher surface in these films.

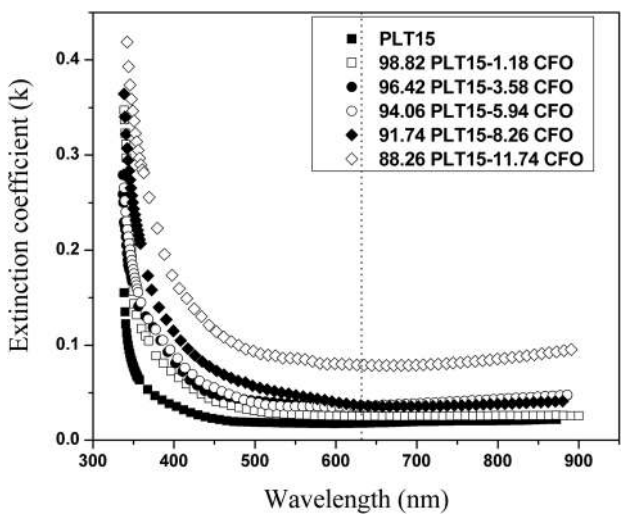

FIG. 5. Plot of (k) as a function of (λ) for PLT15, and (1 − x) PLT15-x CFO composite thin films.

Since the envelope method is not valid is strong absorption region, the calculation of the absorption coefficients of the film needs both the transmission and reflection spectra. For a direct band gap material, the absorption coefficient as a function of photon energy can be expressed as[17]

$$(\alpha hc/\lambda)^2 = \text{Const.}\{(hc)/(\lambda - E_g)\}, \quad (4)$$

where α is the absorption coefficient, (hc/λ) is the incident photon energy, and E_g is the band gap energy. By plotting $(\alpha hc/\lambda)^2$ vs (hc/λ), E_g can be evaluated from the extrapolated linear portion of the plot.

Figure 6(a) shows the $(\alpha h\nu)^2$ vs $(h\nu)$ plots for all these films. Table I and Figure 6(b) show the variation of optical band gap (E_g) with CFO volume contents in (1 − x) PLT15-x CFO composite thin films. It is shown that E_g is systematically reduced with the increase in CFO volume contents. The observed variations are significant and much larger than the experimental uncertainties. The change in the band gap energies of the composite films are probably related to the diffusion of constituent element/(s) from CFO to PLT15 lattice.

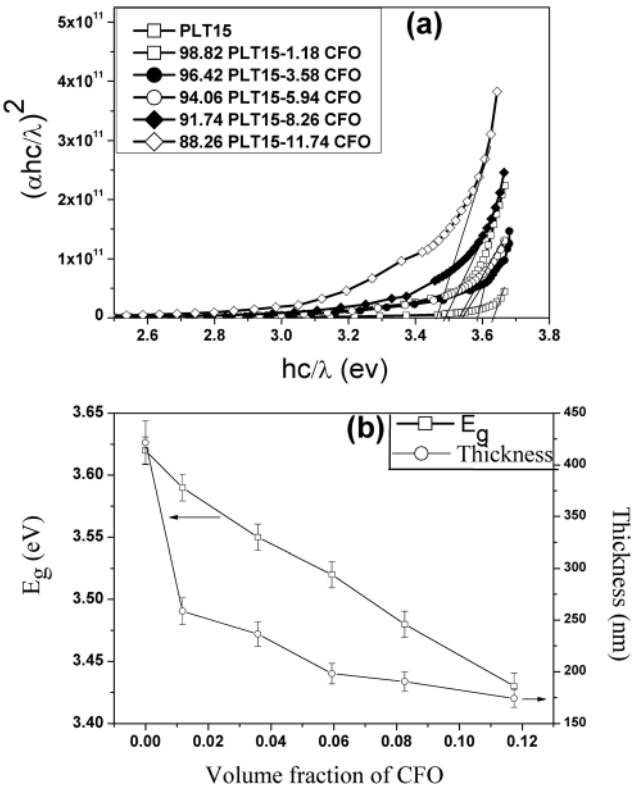

FIG. 6. (a) $(\alpha h\nu)^2$ vs $(h\nu)$ plots for all these films, (b) the variation of optical band gap (E_g) with CFO volume contents and film thickness in $(1-x)$ PLT15-x CFO composite thin films.

We have reported earlier a shift in x-ray diffraction peak with the increase in CFO volume contents in the composite films.[10] The shift is correlated to cation diffusion, resulting the change in lattice parameters. As shown in Fig. 6(b), the thickness of the composite films also reduces with the increase in CFO volume contents. At this point, we are not sure if the reduction of thickness is someway or other related to the observed change in the band gap. More research efforts are required to clarify this issue.

The packing fraction (f) of these films is calculated using effective media approximation. Note that the dielectric constant of PLT15 is high compared to CFO, and also CFO volume fraction is kept low in PLT15 matrix. Therefore, we have tacitly assumed these films to be a single phase dielectric material containing some amount of porosity as second phase. The following relation is used to estimate f:[18]

$$f\frac{n_b^2-n^2}{n_b^2+2n^2}+(1-f)\frac{(1-n^2)}{(1+2n^2)}=0, \quad (5)$$

where n_b and n are the refractive indices of bulk and thin film ferroelectric phase, respectively, whereas f is the fractional porosity.

Table I summarizes these results. Within the limit of the experimental error, we have not noted any major change in the packing fraction of $(1-x)$ PLT15-x CFO composite films.

As a demonstration of validity of our procedures and consistency of values of optical constants derived from it, we use them to calculate the transmission spectra and compare it with experimental data. The agreement between the two, for PLT15 and $(1-x)$ PLT15-x CFO (11.74 vol. %) composite films is shown in Fig. 7. The excellent fit obtained requires only less than 1% change in the thickness values; and in the computed spectra, all the features of the experimental spectra are nicely reproduced.

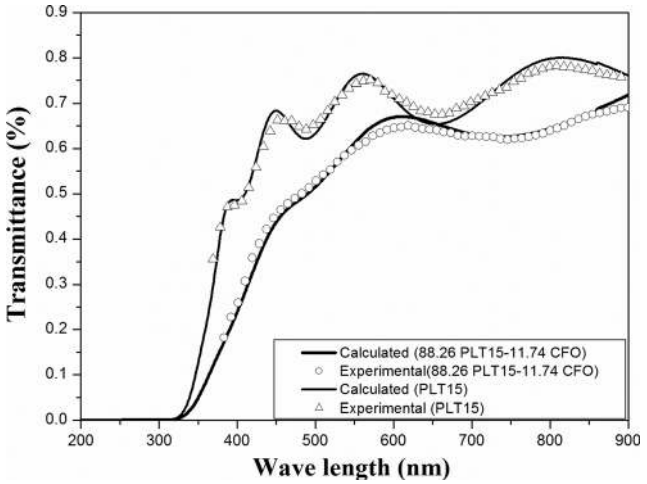

FIG. 7. Computed transmittance data with experimental values for 88.26 PLT15-11.74 CFO composites thin film.

IV. CONCLUSIONS

In the present paper, optical properties of PLT15 and $(1-x)$ PLT15 − xCFO composite thin films are investigated using both transmission and reflection spectra in the wavelength range 200 nm to 900 nm. The refractive index, extinction coefficient, and thickness of these films are determined from the measured transmission spectra. The packing fraction of the film is calculated from its refractive index using effective medium approximation (EMA) and average oscillator strength and wavelength are estimated using Sellmeir type dispersion relation. Absorption coefficient and the band gap energy of each composite film are also calculated. Possible correlations between the nature of CFO phase distribution with band gap energy and other optical properties are discussed.

The following conclusions can be drawn from the present work

- To the best of our knowledge and belief, the optical properties of 0–3 type multiferroic composite thin films have not so far been reported in details. In case of ferroelectric: ferrite based composite films with dilute magnetostrictive phase contents, we have systematically investigated the optical constants of these thin films.
- The refractive index of PLT15 thin film is found to reduce systematically with the increase in CFO volume contents in $(1-x)$ PLT15-x CFO composite films.
- We have demonstrated that analysis of multiferroic composite films in terms of its dispersion of refractive indices could be an effective tool to comment on the magnetostrictive phase distribution in perovskite matrix. Thus in case of 0–3 type $(1-x)$ PLT15-x CFO composite films, we have shown that as long as CFO phase is distributed

homogeneously in PLT15 matrix, the measured refractive indices follow Sellmeir dispersion formalism. Interestingly, for percolative magnetostrictive phase (CFO) distribution, the refractive index variation of the composite films deviates from the Sellmeir type dispersion (for one dominant electronic oscillator).

- The low values of the extinction coefficients and the appearance of fringes both in transmittance and reflectance spectra indicate reasonably good surface smoothness and excellent thickness uniformity of these sol-gel derived 0–3 type multiferroic composite films.
- The thickness values obtained from these simple optical measurements and allied data analyses compare well with the thickness data measured by commercial dedicated instrument.
- Increase of the CFO volume contents in $(1-x)$ PLT15-x CFO composite films does not have any appreciable effect on the estimated packing fraction.
- We have reported a systematic reduction of the band gap energy in $(1-x)$ PLT15-x CFO composite films with the increase in CFO volume contents.

[1]G. H. Haertling, in *Piezoelectric and Electro Optic Ceramics, in Ceramic Materials for Electronics*, edited by R.C. Buchanon (Marcel Dekker, New York, 1986), p. 139.
[2]S. Bhaskar, S. B. Majumder, E. R. Fachini, and R. S. Katiyar, J. Am. Ceram. Soc. **87**, 384 (2004).
[3]W. J. Leng, C. R. Yang, J. H. Zhang, H. W. Chen, and J. L. Tang, J. Appl. Phys. **100**, 083505 (2006).
[4]S. Iakovlev, C.-H. Solterbeck, M. Kuhnke, and M. Es-Souni, J. Appl. Phys. **97**, 094901 (2005).
[5]W. Bai, Y. Q. Gao, Y. Zhu, X. J. Meng, T. Lin, J. Yang, Z. Q. Zhu, and J. H. Chu, J. Appl. Phys. **109**, 064901 (2011).
[6]A. Kumar, R. C. Rai, N. J. Podraza, S. Denev, M. Ramiez, Y.-H. Chu, L. W. Martin, J. Ihlefeld, T. Heeg, J. Schubert, D. G. Schlom, J. Orenstein, R. Ramesh, R. W. Collins, J. L. Musfeldt, and V. Gopalan, Appl. Phys. Lett. **92**, 121915 (2008).
[7]J. M. Park, F. Gotoda, T. Kanashima, and M. Okuyama, J. Korean Phys. Soc. **59**, 2537 (2011).
[8]H. Shima, T. Kawae, A. Morimoto, M. Matsuda, M. Suzuki, T. Tadokoro, H. Naganuma, T. Iijima, T. Nakajima, and S. Okamura, Jpn. J. Appl. Phys., Part 1 **48**, 09KB01 (2009).
[9]T. Choi, S. Lee, Y. J. Choi, V. Kiryukhin, and S.-W. Cheong, Science **324**, 63 (2009).
[10]S. Roy and S. B. Majumder, Phys. Lett. A **375**, 1538 (2011).
[11]S. Roy, R. Chatterjee, and S. B. Majumder, J. Appl. Phys. **110**, 036101 (2011).
[12]J. C. Manifacier, J. Gasiot, and J. P. Fillard, J. Phys. E: Sci. Instrum. **9**, 1002 (1976).
[13]R. Swanepoel, J. Phys. E: Sci. Instrum. **16**, 1214 (1983).
[14]S. Bhaskar, S. B. Majumder, M. Jain, P. S. Dobal, and R. S. Katiyar, Mater. Sci. Eng. B **87**, 178 (2001).
[15]J.–C. Ho, I.-N. Lin, and K.–S. Liu, J. Mater. Sci. **29**, 1884 (1994).
[16]M. Didomenico, Jr. and S. H. Wemple, J. Appl. Phys. **40**, 720 (1969).
[17]U. Pal, S. Saha, A. K. Chaudhary, V. V. Rao, and H. D. Banerjee, J. Phys. D **22**, 965 (1989).
[18]D. A. G. Bruggeman, Ann. Phys. (Leipzig) **24**, 636 (1935).
[19]See supplemental information at http://dx.doi.org/10.1063/1.4747918 for information on the method to estimate the optical constants of transparent optical films deposited on optically transparent and flat substrates.